SEMARAK ILMU PUBLISHING

Journal of Advanced Research in Numerical Heat Transfer

Journal homepage:
https://semarakilmu.com.my/journals/index.php/arnht/index
ISSN: 2735-0142

Computational Fluid Dynamics Analysing of Preferential Flow in Gas Mask Filter Cartridge

Muhammad Hazimuddin Halif[1], Nor Azali Azmir[2], Ishkrizat Taib[2,*], Nor Mohd Razif Noraini[3]

[1] Faculty of Mechanical and Manufacturing, Universiti Tun Hussein Onn Malaysia, 86400 Batu Pahat, Johor, Malaysia
[2] Department of Mechanical Engineering, Faculty of Mechanical Engineering and Manufacturing, Universiti Tun Hussein Onn, 86400, Parit Raja, Batu Pahat, Johor, Malaysia
[3] National Institute of Occupational Safety and Health (NIOSH), 43650 Bandar Baru Bangi, Selangor, Malaysia

ARTICLE INFO

Article history:
Received 9 June 2024
Received in revised form 12 July 2024
Accepted 19 August 2024
Available online 30 September 2024

Keywords:
Gas mask filtration; Main sieve passageway; CFD

ABSTRACT

In various hazardous locations, gas mask filters are essential to protect from airborne pollutants and harmful gases. However, under certain conditions, such as the weather or climate in some locations can affect gas mask filtration. Based on a previous study, the existing geometry of the gas mask filter cartridge unit been analysed for its preferential flow within the gas mask domain, which resulted in a significant pressure drop and heat concentration in the filter, affecting the filtration. However, another study suggested designing the main sieve passageway of the filter to help in resolving the pressure drop and create much well distribution of flow within the cartridge. In this study, three geometries with re-design of the main sieve passageway of the filter were made and simulated to determine the preferential flow using the computational fluid dynamics (CFD) method. Two filter concentrations (300 ppm, and 1000 ppm) and constant humidity ratios of at 80 % were simulated. The presence of the dead zone was examined using the computational fluid dynamics (CFD) method, which was controlled by the Navier-Stokes equation and continuity based on several flow parameters. Based on the result occupied can be concluded, the second geometry had a much better velocity contour distribution around 40% than the other geometry, maintaining the overall minimum velocity area even though the formation of the dead zone area for the second geometry was 10% higher at the lower part of the filter than for the third geometry. The abilities of the second geometry to perform well even in the presence of higher concentrations brought to the honeycomb-based design as the main sieve passageway actually improve the velocity distribution and then minimizing formation of "dead zone". Concluding justified that the proposed geometry met the prediction of improving the pressure drop and create quite well distribution of flow in the filter. prediction of improving the pressure drop and create quite much well distribution of flow in the filter.

1. Introduction

It has been made clear that any industrial sector involved in poisonous or polluting gas vapour environmental worksite should wear protective equipment that is appropriate for their existing

* *Corresponding author.*
E-mail address: iszat@uthm.edu.my (Ishkrizat Taib)

https://doi.org/10.37934/arnht.24.1.5868

conditions. The gas mask filter, which aids in protecting the respiratory system from inhaling hazardous and toxic substances, is a piece of safety equipment that must be used. The Institute of Occupational Safety and Health (NIOSH), which regularly monitors employee exposure to dangerous gas vapour environments, especially in the oil and gas industries [1,2], also oversees this part of equipment as mandatory. Based on reports, a worker dies of toxic exposure in the workplace every 30 seconds, and one of the causes is failing to provide protective gear for workers [3,4]. This comes as an alert to the employer especially regarding having a suitable and recognise gear protective that approved by the authorities for protecting workers health and safety within the working environment. A gas mask usually comprises a set of filters that manage to filter out any toxins throughout a layer of part that filters air flowing through it. This has mostly been done using porous materials that capture the substance that flow with the air, and basically, the material of porous media is based on the type of substance it will be filtered for [5-7].

However, frequent absorption of the gas mask filter in the pollutant's environment and exposure to humid climates speed up the expiry date of the filter even though the expiry date set by the manufacturer is permissible [8,9]. Additionally, the commercial gas mask filter's huge surface area resulted in a low absorption rate through the filter paper and activated carbon, which also decreases the filter lifetime [10-14]. Based on a previous study by Noraini *et al.,* [15] they used Computational Fluid Dynamics in assess the impact of temperature and relative humidity in Malaysia on gas mask filtration. Their methodology involved simulating the airflow distribution using the Navier-Stokes equations to model fluid dynamic heat transfer in the filter medium. They applied different humidity and concentration levels in order to find areas with severeness that formed dead zones in the filter medium, suggesting a possibility of increasing the pressure drop. The findings showed the critical area of pressure drop formed at the charcoal bed material as the humidity ratio increased, which had a substantial effect on the velocity distribution of flow overall. These results indicates that current cartridges are not performing well within the local climate and create a problem related to preferential flow.

In the meantime, the suggestion from previous studies reveals there are ways that filtration of the gas mask cartridge can be improved by redesigning the main sieve passageway that helps re-distribute the air flow much evenly [16,17]. The filter geometry can be modified to increase the absorption rate of the filtered and activated carbon. In order to determine the direction of the overall improvement of the filter flow, the aerodynamic characteristics of the designed filter based on the preferential flow entering the filter was examined. Three different gas mask filter geometries were deemed suitable for testing with a honeycomb structure [18,19]. The CFD method is useful for assessing the flow variables in porous media within a gas filter, and it can also be used to evaluate the geometry's performance according to the parameter stated [20,21].

2. Methodology

2.1 Geometry of the Difference Gas Mask Filter

The geometrical modelling for the gas mask was developed using a commercially aided (CAD) software called SOLIDWORKS 202. In this study, three different gas mask filters were developed and simulated. A 3-dimensional model of the variation gas mask filter is shown in Figure 1.

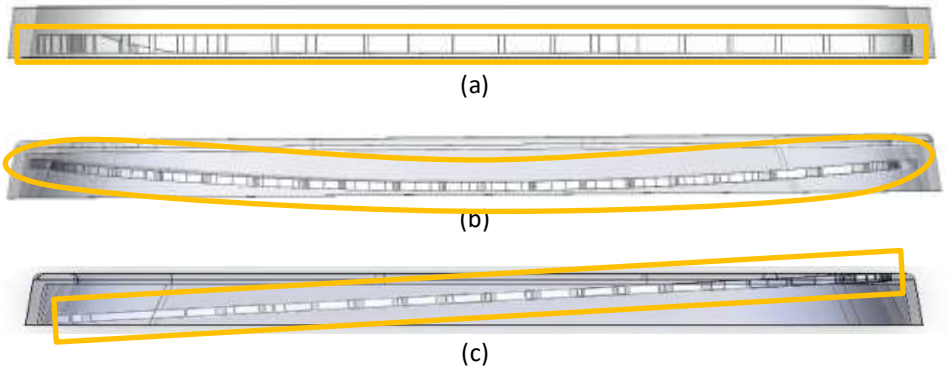

Fig. 1. Geometries of the main sieve passageway (a) Flat plane shape for the first model, (b) Curve-plane shape for the second model, (c) inclined plane shape for the third model

2.2 Discretization Technique

ANSYS FLUENT 23 manages to analyse multiple, automated parametric designs without complex programming. The proposed software includes various physical models that capture many types of phenomena related to fluid flow. The proposed solver is based on the finite volume method with several types of arbitrary mesh topologies, such as hexahedral, tetrahedral, wedge, and pyramid elements. Additional mesh refinement is employed for specified porous media at the filter surfaces during calculation. The time derivatives are approximated with implicit second-order accuracy in both space and time. The proposed method allows the use of larger time steps and provides better stability. Both the velocity inlet and pressure outlet were computed to solve the continuity and Navier-Stokes equations. The physical law describing the problem of a gas mask is the conservation of mass, the conservation of momentum as stated in Eq. (1) and Eq. (2);

$$\nabla . V = 0 \tag{1}$$

$$\frac{dV}{dt}\rho = -\nabla P + \mu\nabla^2 V \text{ -}\nabla P\text{+ }\mu\nabla\text{^2 V} \tag{2}$$

where is ρ air density, P is pressure, μ is the air viscosity, and V is the air velocity.

2.3 Meshing of the Gas Mask Model

As seen in Figure 2, a mesh of the gas mask model and details at the inlet and outlet is shown also 4,354,230 elements and 767,576 nodes have been used to mesh the whole structure.

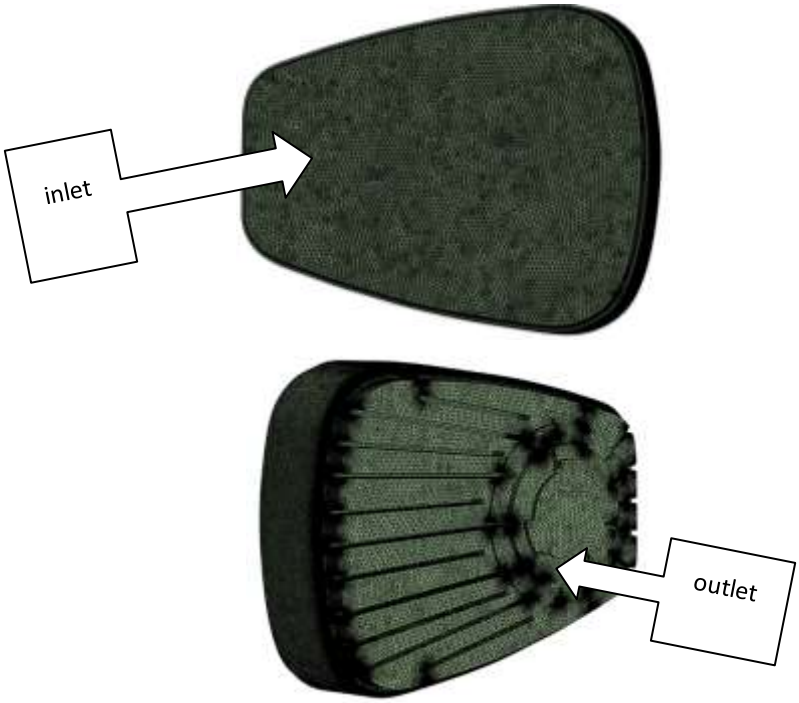

Fig. 2. Meshed model of the gas mask

2.4 Parameter Assumptions and Boundary Conditions

The canister inlet maintained a steady inhalation flow rate throughout all simulations. Because the inlet area was fixed, the mean velocity was calculated according to the inlet boundary. The reference pressure (1 atm) at the inlet was constant. The outlet boundary condition was the pressure outlet boundary. The no-slip condition was assumed for all solid walls. This filter is in contact with a natural heat source from the environment. The inlet air is approximately 1000 m3/h for flow rate, and the inlet temperature is 30℃. In the inner space of the filter part of the model, water vapour is considered with a humidity of 80% based on the Malaysian relative humidity range defined for the flowing fluid. The energy model was activated, and the SST k-omega model with the use of a standard wall function was exploited for fluid flow analysis. The concentrations used for these conditions were 300 and 1000 ppm. The material properties of density, specific heat capacity, thermal conductivity, and viscosity are listed in Table 1 below.

Table 1
Material properties

Material	Air
Density (kg.m-3)	1.225
Specific heat (j.kg-1. K-1)	1000
Thermal conductivity (W.m-1. K-1)	0.0242
Viscosity (kg.m-1. s-1)	0.000017894

2.5 Porous Media Parameters

The simulation of the gas filter involves the parameters of porous media in which the pressure drop in the gas filter normally comes from the filter paper and activated carbon. A Reynold number of 78,000 was used in this simulation. Both viscosity and inertial effects were considered. Thus, the

Wertheimer equation was adopted to describe the momentum dissipation through the porous media, as stated in the equation;

$$-\frac{\Delta P}{L} = \alpha \mu V_s + \beta \rho V_s^2 \quad (3)$$

where α is the reciprocal permeability of the porous material (or viscosity parameter. β is usually called the inertial parameter. ΔP is the pressure drop in the porous medium zone. Here, is the length of the flow direction; μ is the fluid viscosity. Vs denotes the superficial velocity of the fluid entering the porous medium zone. The filter paper and activated carbon used in the rfp-1000 gas filter are consistent with the literature. Therefore, the coefficients of the filter layer and activated carbon layer were are consistent with the literature. The coefficients for the filter layer and activated carbon layer were determined as follows:

$$\alpha_1 = 2.19 \times 10^9 m^{-2}, \beta_1 = 7.5 \times 10^4 m^{-1} \quad (4)$$

The coefficients of the activated carbon layer are determined as:

$$\alpha_2 = 2.19 \times 10^9 m^{-2}, \beta_2 = 7.5 \times 10^4 m^{-1} \quad (5)$$

3. Results

3.1 Pressure Drop on Gas Mask Filter Concentration Under Local

Table 1 shows the impact of pressure drop on the gas filter at different humidity. The pressure drop distributions for various gas mask filter models under 80% humidity with 300- and 1000-ppm concentrations are shown. Based on these results, the pressure drop gradually increased from the upper side as concentrations rose, and with the exception of Model C, the pressure drop was more pronounced on the left side than on the right side of the charcoal filter. This can be linked to left side flow streamline recirculation, which causes momentum loss, radial flow disturbance, and the creation of a dead zone. For Model A, which corresponds to 80% humidity at concentrations of 300 ppm and 1000 ppm, the largest pressure decrease was observed among the studied settings. Compared with the surface boundary, the pressure drop also affected a wider area of the charcoal filter. These results are consistent with earlier studies [8].

Further investigation revealed that the pressure decrease for Model A occupies a larger portion of the filter than the other regions. With a rise in the filter concentration and humidity ratio, the pressure decreases exhibit a significant increase. Model B shows significantly less pressure decline across the filter region, which a lesser decrease in the adsorption rate and a marginally less problematic time for gas breakthrough.

A non-significant pressure drop is observed in the middle of the filter at the same time for geometry 3. Instead, where the air flow enters the filter at the bottom of the filter is where there is a somewhat larger pressure drop. The filter's minor slope or descent from the upper section, which caused pressure to concentrate and build up at the bottom of the filter, is an obvious explanation. It should be remembered that dry air and water vapour have different densities at the same temperature. As a result, excessive humidity tends to make the air less dense, thereby lowering its pressure [8].

Table 1
Pressure drop distribution in (a) Model A, (b) Model B, (c) Model C

	Model A	Model B	Model C
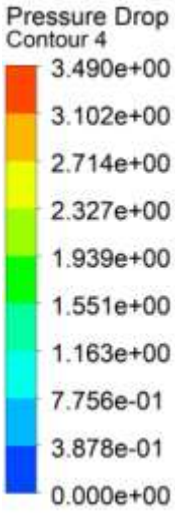	30C, 80%, and 300 ppm	30C, 80%, and 300 ppm	35C, 80%, and 300 ppm
	30C, 80%, and 1000 ppm	30C, 80%, and 1000 ppm	30C, 80%, and 1000 ppm

3.2 Heat Propagation Effect Under Different Concentrations

An increase in local temperature within the filter layer caused the water vapour ratio to increase. This is because water vapour has a propensity to trap heat, particularly in the charcoal filter shown in Table 2. However, the results show that for various water ratios and concentrations, there is not much variance in the temperature differential at the filter layer among the different models. This is a result of the charcoal filter's porous structure, which evenly distributed the temperature across the filter. Table 2 shows that the average temperature occupies approximately 80% of the space in the gas mask filter. Despite the similar temperature values, the high humidity in the area caused a reduction in the filter's impedance of flow in terms of concentration.

Table 2
Distribution of temperature (a) Model A, (b) Model B, (c) Model C

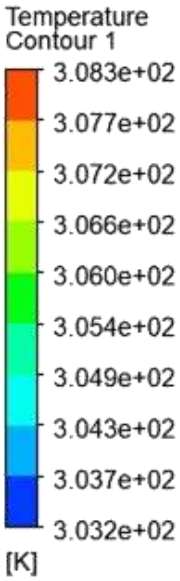

Model A	Model B	Model C
30C, 80%, and 300 ppm	30C, 80%, and 300 ppm	30C, 80%, and 300 ppm
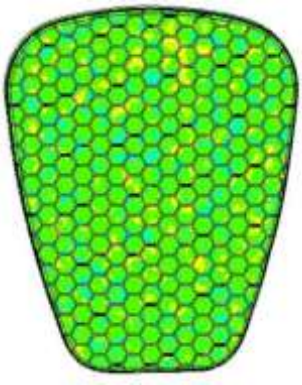	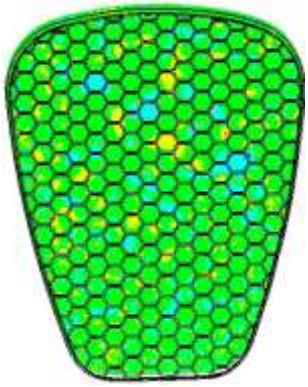	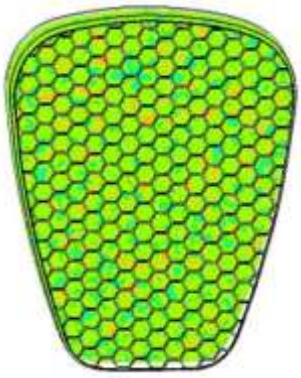
30C, 80%, and 1000 ppm	30C, 80%, and 1000 ppm	30C, 80%, and 1000 ppm
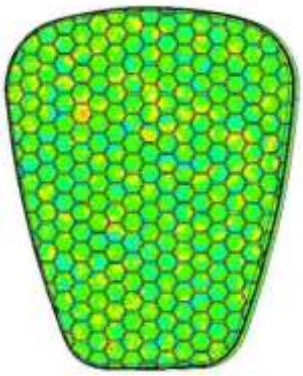	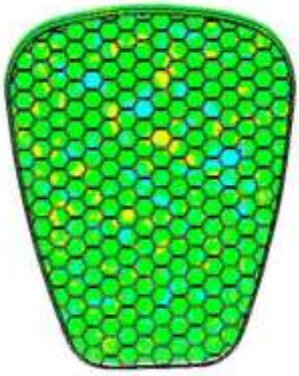	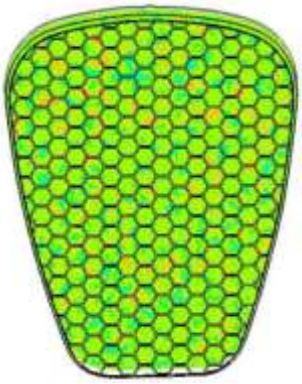

The results further demonstrate that the local temperature plays a function in the increase in water vapour ratio while considering the identical parameters as previously described. However, despite the variations in geometry and environmental conditions, the temperature distribution within the filter layer remained largely constant. This is largely due to the charcoal filter's porous medium effect. Due to the significant humidity, this homogeneous temperature distribution affects the total heat propagation across the filter, which is affected by the high humidity present in the local environment [8].

3.3 Velocity Effect on The Low-Concentrated Filter Under The High Humidity Condition

The fluid and particles are slightly difficult to pass through the region of low velocity for a porous medium filter, especially in humid climates (refer Table 3). This phenomenon normally occurs due to increases the pressure and temperature in the charcoal filter, which are prone to decrease the efficiency of the filtration. The results show that flow re-circulation was observed in all geometry of the gas mask, where flow re circulation was presented as negative values, as shown in most of the Model. This result is due to the increase in the superficial velocity at the inlet, which is prone to form a dead zone. The region of the dead zone corresponding to the worst adsorption rate of the charcoal filter.

Table 3
Distribution of velocity (a) Model A, (b) Model B, (c) Model C

	Model A	Model B	Model C
	30C, 80%, and 300 ppm	30C, 80%, and 300 ppm	30C, 80%, and 300 ppm
	30C, 80%, and 1000 ppm	30C, 80%, and 1000 ppm	30C, 80%, and 1000 ppm

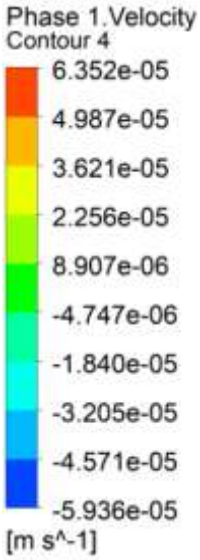

From the observation, Model A gas mask filter showed low-flow re-circulation was formed around the of the filter at the 300-ppm concentration and evenly distributed with an increase in the filter concentration and humid condition. However, Model B showed a much better distribution even though there was formation of restrict flow at the bottom, but the overall flow was not affected even at higher concentrations. On the other hand, Model C, even at the 300-ppm concentration, showed an impressive velocity distribution, but as the concentration increased the overall velocity distribution upwards from below region started to restrict and reduce the flow velocity. The constant velocity distribution was also observed on the centre side of the filter compared to the other regions of the charcoal filter. This result is due to fluid flow passing through the porous medium of the charcoal filter without resistance compared to other regions. In the same time, the different geometry gives different ways of flow distribution that alter the formation of flow restriction, which even increases the concentration still does not disturb other regions of the filter.

3.4 Validation of Results

From a previous study (Noraini *et al.,* [15]), the preferential flow for a gas mask canister was simulated. Figure 3 shows a comparison of the pressure drop and velocity distribution results the previous study. Model B, where the curve geometry was selected because the overall performance with previous filter were better.

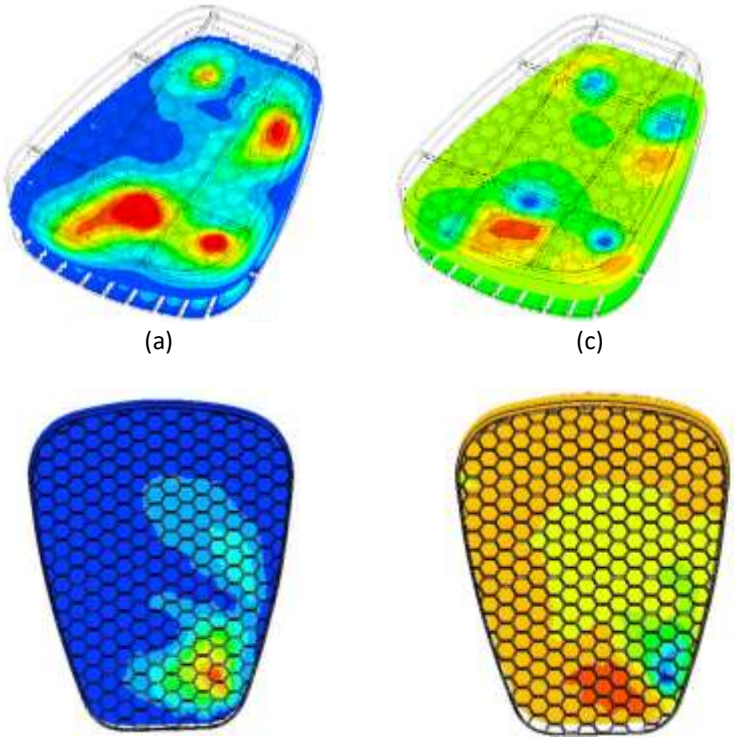

Fig. 3. Comparison between results where a) Pressure drop in previous study, b) Pressure drop in Model B, c) Velocity in previous study with, d) Velocity in Model B

From Figure 3, the results from the simulations are different from those from previous studies, where different pressure drops or dead zone formation occur within the Model with the improved distribution of velocity. This is due to the Model that brought a much wider distribution of flow and reduced air re-circulation from influencing the overall velocity. Thus, the Model of the honeycomb main sieve-passageway does improve the current Model filter.

4. Conclusions

Analysis is done on the gas mask filters where the overall flow at three different geometries of the gas mask filter still had the formation of dead zone; however, compared to the existing geometry, there had been improvement in terms of velocity distribution. The investigation on the effect of local climate or humidity in the air on gas mask filtration been seen where the result of the temperature distribution on the charcoal filler were through evenly, the high humidity ratio and pressure drop in the gas mask filter still happens in the form of a dead zone of pressure drop that can reduce the efficiency of filter concentration overall as time goes by. The gas mask filter's lifespan will be shortened at the same time by the high humidity ratio in the filter, which will trap heat inside the filter, causing a pressure drop. By analysing the air flow characteristic towards the gas mask filtration using Fluent analysis had showed the pressure drop was noticeable when high velocity circulation occurred near the charcoal filter. The contour of velocity also showed distribution through the gas mask filter, especially for geometry 2, exhibiting greater absorption with better velocity distribution and less pressure drop or dead zone generation overall.

Acknowledgement

This research was supported by the University of Tun University Tun Hussein Onn Malaysia (UTHM) for GPPS Vot Q562. Communication of this research is made possible through monetary assistance by Universiti Tun Hussein Onn Malaysia and the UTHM Publisher's Office via Publication Fund E15216.

References

[1] Witter, Roxana Z., Liliana Tenney, Suzanne Clark, and Lee S. Newman. "Occupational exposures in the oil and gas extraction industry: State of the science and research recommendations." American journal of industrial medicine 57, no. 7 (2014): 847-856. https://doi.org/10.1002/ajim.22316

[2] Esswein, Eric J., John Snawder, Bradley King, Michael Breitenstein, Marissa Alexander-Scott, and Max Kiefer. "Evaluation of some potential chemical exposure risks during flowback operations in unconventional oil and gas extraction: preliminary results." Journal of Occupational and Environmental Hygiene 11, no. 10 (2014): D174-D184. https://doi.org/10.1080/15459624.2014.933960

[3] ISHN. (2019, March 15). A worker dies of toxic exposure in the workplace every 30 seconds. ISHN RSS. https://www.ishn.com/articles/110415-a-worker-dies-of-toxic-exposure-in-the-workplace-every-30-seconds.

[4] Tran, Phuong Thi Minh, Jie Rui Ngoh, and Rajasekhar Balasubramanian. "Assessment of the integrated personal exposure to particulate emissions in urban micro-environments: A pilot study." Aerosol and Air Quality Research 20, no. 2 (2020): 341-357. https://doi.org/10.4209/aaqr.2019.04.0201

[5] Kiani, Sidra Shaoor, Amjad Farooq, Masroor Ahmad, Naseem Irfan, Mohsan Nawaz, and Muhammad Asim Irshad. "Impregnation on activated carbon for removal of chemical warfare agents (CWAs) and radioactive content." Environmental Science and Pollution Research (2021): 1-18. https://doi.org/10.1007/s11356-021-15973-1

[6] Mohammad-Khah, A., and R. Ansari. "Activated charcoal: preparation, characterization and applications: a review article." Int J Chem Tech Res 1, no. 4 (2009): 859-864.

[7] Harati, Bahram, Seyed Jamaleddin Shahtaheri, Ali Karimi, A. Z. A. M. Kamal, Alireza Ahmadi, Maryam Afzali Rad, and Ali Harati. "Evaluation of respiratory symptoms among workers in an automobile manufacturing factory, Iran." Iranian Journal of Public Health 47, no. 2 (2018): 237.

[8] Abiko, Hironobu, Mitsuya Furuse, and Tsuguo Takano. "Application of Wheeler–Jonas equation and relative breakthrough time (RBT) in activated carbon beds of respirator gas filters." Air Quality, Atmosphere & Health 13 (2020): 1057-1063. https://doi.org/10.1007/s11869-020-00857-z

[9] Brochocka, Agnieszka, and Krzysztof Makowski. "General Guidelines for the Selection and Use of Filtering Respiratory Protective Devices." In Nanoaerosols, Air Filtering and Respiratory Protection, pp. 199-213. CRC Press, 2020. https://doi.org/10.1201/9781003050070-8

[10] Ligotski, Roman, Uta Sager, Ute Schneiderwind, Christof Asbach, and Frank Schmidt. "Prediction of VOC adsorption performance for estimation of service life of activated carbon based filter media for indoor air purification." Building and Environment 149 (2019): 146-156. https://doi.org/10.1016/j.buildenv.2018.12.001

[11] Si, Fangfang, Pengfei Lian, Derui Yang, Guolin Han, Shaoyue Hao, and Pingwei Ye. "3D numerical simulation of aerodynamic characteristics of a gas filter." Journal of Applied Mathematics and Physics 7, no. 8 (2019): 1920-1928. https://doi.org/10.4236/jamp.2019.78132

[12] Kim, Min-Wook, Young-Soo Kim, and Yong-Hwan Park. "Pressure Loss in Canisters with Conditions of Activated Carbon Particles." Fire Science and Engineering 31, no. 4 (2017): 7-11. https://doi.org/10.7731/KIFSE.2017.31.4.007

[13] Wood, Samuel GA, Nilanjan Chakraborty, Martin W. Smith, and Mark J. Summers. "A computational fluid dynamics analysis of transient flow through a generic Chemical Biological Radiological and Nuclear respirator canister." Chemical Engineering Research and Design 142 (2019): 13-24. https://doi.org/10.1016/j.cherd.2018.11.028

[14] Jeon, Rakyoung, Shin Hyuk Kim, Kwangjun Ko, Kihyun Kwon, Myungkyu Park, Ireh Seo, Min Oh, and Chang-Ha Lee. "Advanced cartridge design for a gas respiratory protection system using experiments, CFD simulation and virtual reality." Journal of Cleaner Production 426 (2023): 139101. https://doi.org/10.1016/j.jclepro.2023.139101

[15] Noraini, NM Razif, Nor Azali Azmir, Ishkrizat Taib, Amir Abdullah Muhamad Damanhuri, Mohd Idain Fahmy Rosley, and Azil Bahari Alias. "Analysis of Preferential Flow at the Front Mesh Cartridge of the Gas Mask Filter: Cases in Malaysia Climate Environment." Journal of Advanced Research in Applied Sciences and Engineering Technology 28, no. 3 (2022): 299-311. https://doi.org/10.37934/araset.28.3.299311

[16] Magomedov, I. A., and Z. S. Sebaeva. "Comparative study of finite element analysis software packages." In Journal of Physics: Conference Series, vol. 1515, no. 3, p. 032073. IOP Publishing, 2020. https://doi.org/10.1088/1742-6596/1515/3/032073

[17] Schulte, Paul, Charles Geraci, Ralph Zumwalde, Mark Hoover, and Eileen Kuempel. "Occupational risk management of engineered nanoparticles." Journal of occupational and environmental hygiene 5, no. 4 (2008): 239-249. https://doi.org/10.1080/15459620801907840

[18] Su, Yin-Chia, and Chun-Chi Li. "Computational fluid dynamics simulations and tests for improving industrial-grade gas mask canisters." Advances in Mechanical Engineering 7, no. 8 (2015): 1687814015596297. https://doi.org/10.1177/1687814015596297

[19] Tripathi, L., and B. K. Behera. "3D woven honeycomb composites: Manufacturing method, structure properties, and applications." J Textile Eng Fashion Technol 8, no. 3 (2022): 71-74. https://doi.org/10.15406/jteft.2022.08.00304

[20] Abdessemed, Chawki, Yufeng Yao, Abdessalem Bouferrouk, and Pritesh Narayan. "Morphing airfoils analysis using dynamic meshing." International Journal of Numerical Methods for Heat & Fluid Flow 28, no. 5 (2018): 1117-1133. https://doi.org/10.1108/HFF-06-2017-0261

[21] Permadi, N. V. A., J. H. Chen, and E. Sugianto. "Influence of Full and Symmetrical Domains on the Numerical Flow around a SUBOFF Submarine Model using Open FOAM." Journal of Applied Fluid Mechanics 16, no. 5 (2023): 1017-1029. https://doi.org/10.37934/cfdl.16.1.107120